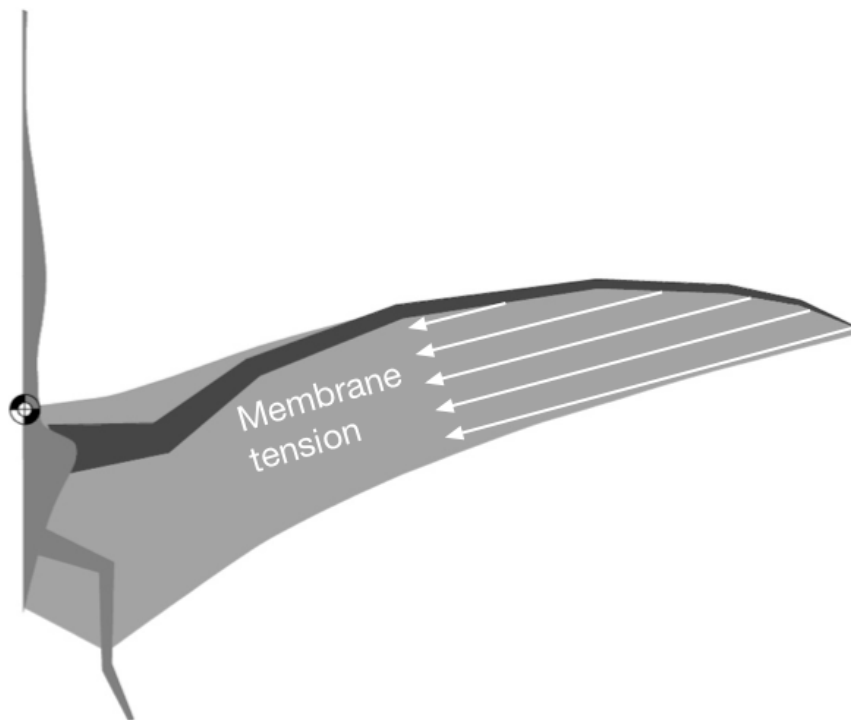
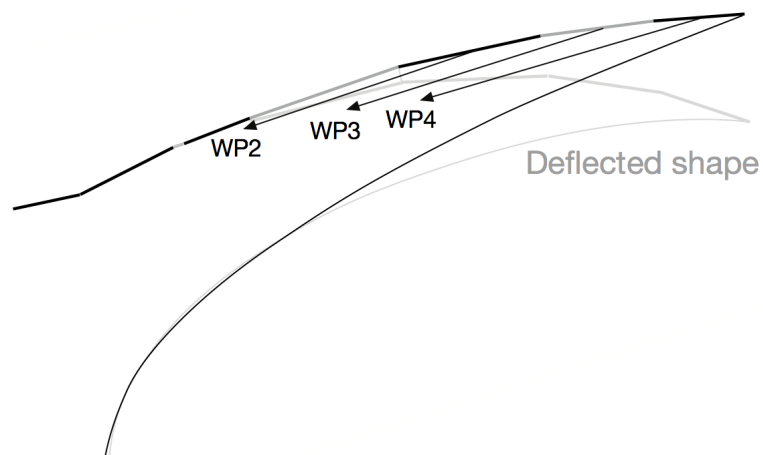


**Figure 6.1**



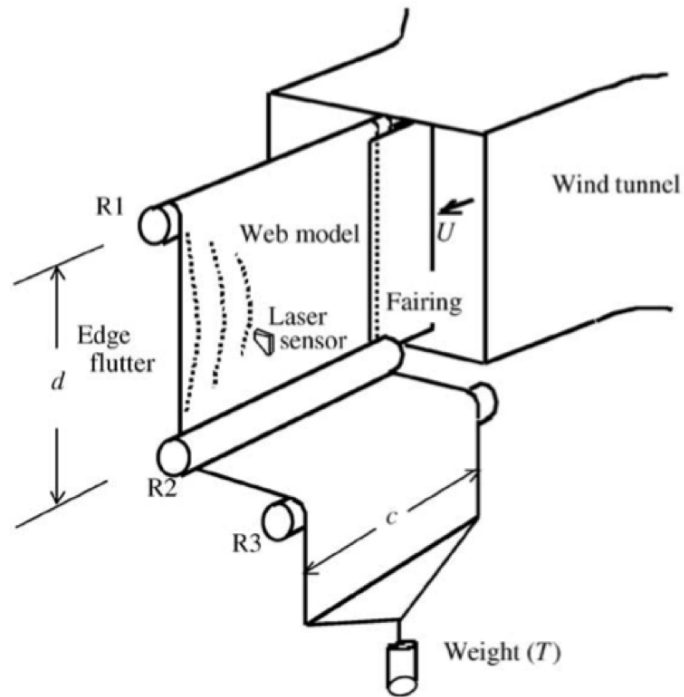
Simple model of membrane tension, assuming it is constant across the width of the wing at the Mc4/WP1 joint. Consequently, the tension must be reacted by forces in the proximal membrane.

**Figure 6.2**



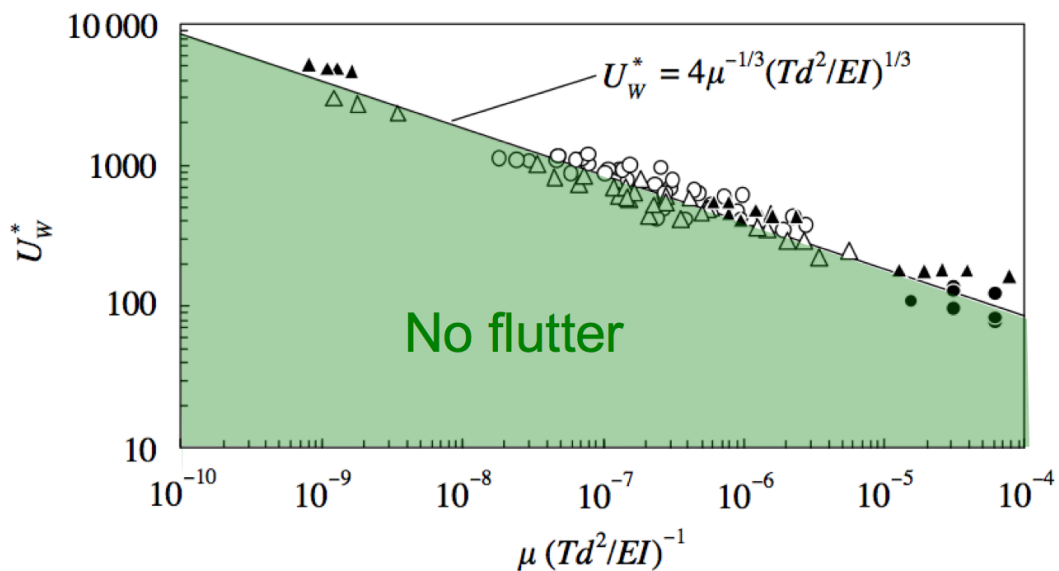
More complex model of membrane tension, assuming it is concentrated anteriorly, which corresponds to the distribution of lift force pressure across the wing chord. In this model, most of the tension is contained with the "bow" formed by the wing spar from the elbow to the wing tip, so reacted by wing bones rather than the proximal membrane.

**Figure 6.3**



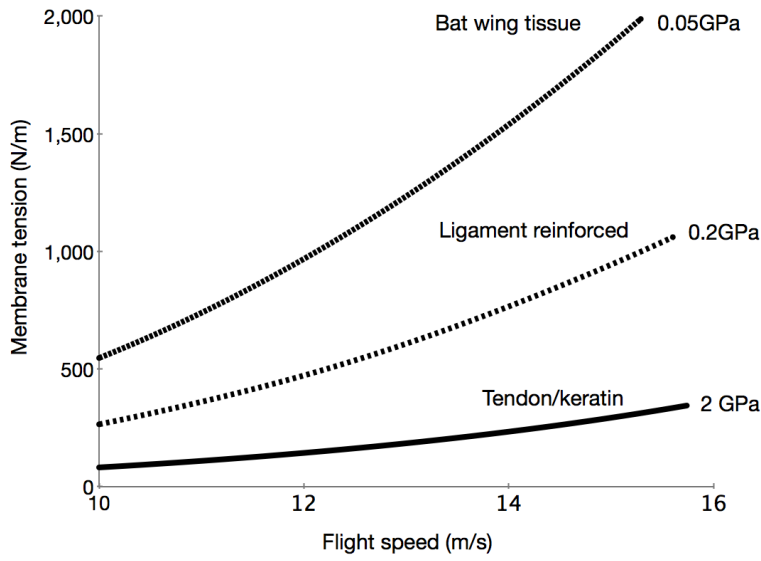
Sketch copied from Watanabe (2002). Air flow from a wind tunnel is directed across a tensioned membrane with a chord  $c$  and span  $d$ , subjected to a tension applied by the suspended weight.

**Figure 6.4**



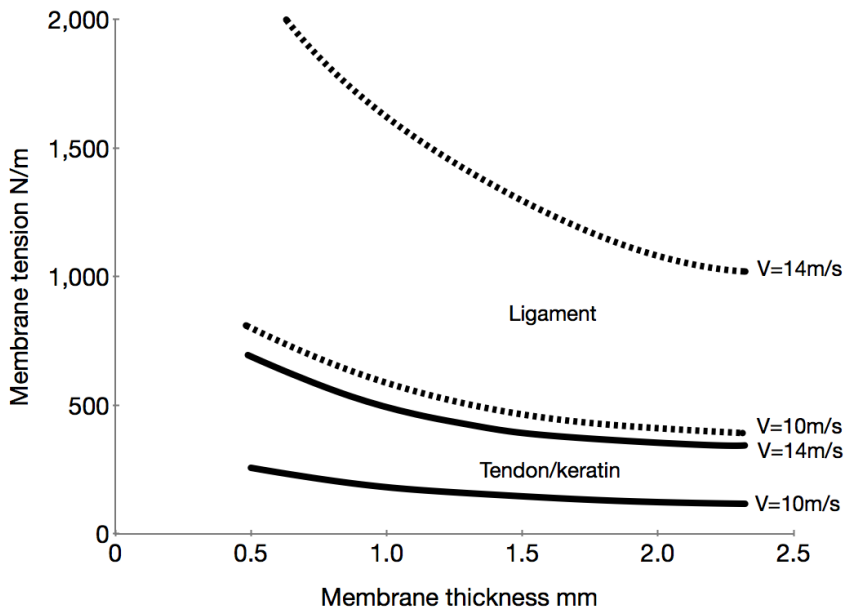
Results of the flutter tests (combined with data from other sources.) From Watanabe (2002). The results show a clear boundary between conditions where flutter occurs and those where it does not. For details of the derivation of the variables, see text.

**Figure 6.5**



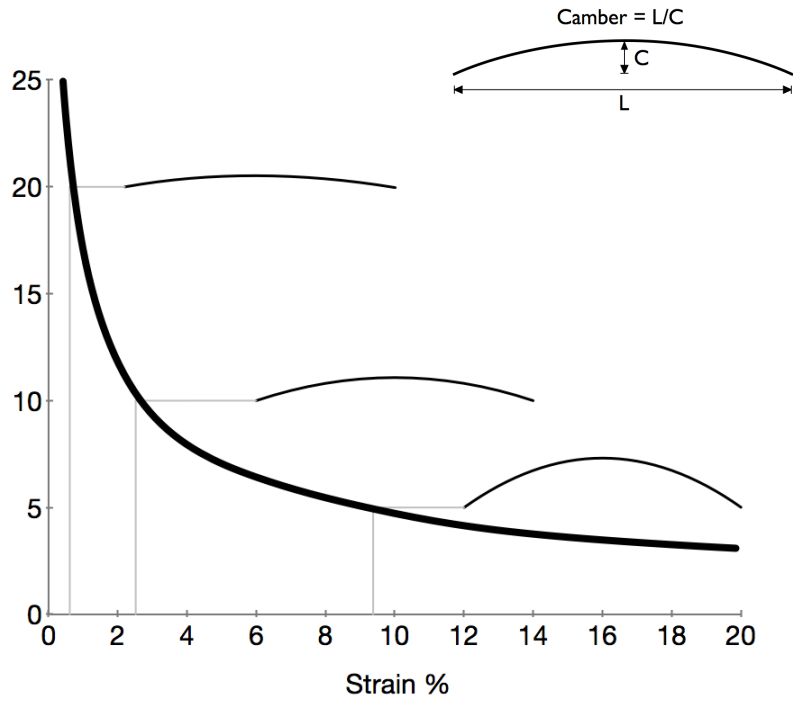
Membrane tension required to suppress flutter. The required tension varies with the stiffness of the membrane and the flight speed (other factors being held constant). Increasing material modulus reduces the required tension and/or extends the achievable flight speed range for a given tension.

**Figure 6.6**



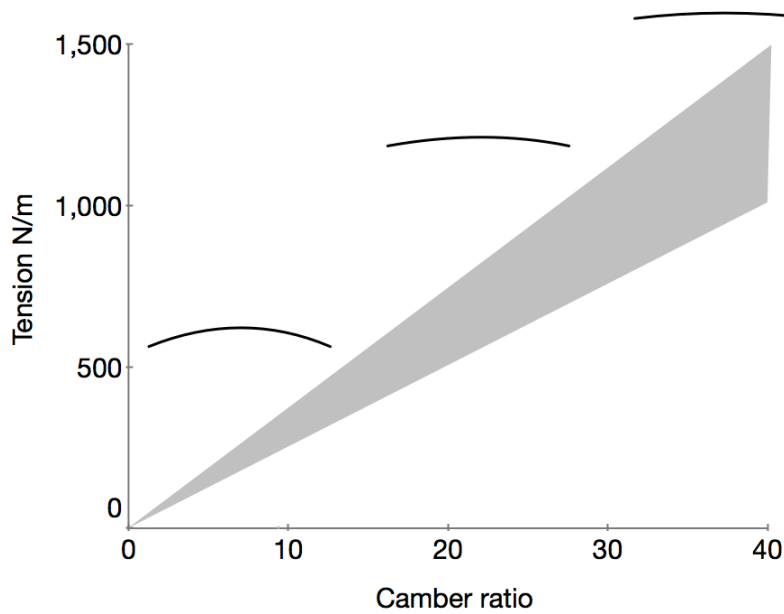
Effect of membrane thickness on required tension at two different flight speeds. Material properties as in Figure 6.5

**Figure 6.7**



Variation of section camber with membrane strain. Camber is defined as the ratio of the width ( $L$ ) of the membrane and the deflection ( $C$ ).

**Figure 6.8**



Variation of camber due to aerodynamic forces with membrane tension. The shaded area represents the likely range of body mass and the results are for a high tensile membrane.